Dalton Transactions

Accepted Manuscript

ROYAL SOCIETY OF CHEMISTRY

www.rsc.org/dalton

Dalton Transactions

Dynamic Article Links ►

Cite this: DOI: 10.1039/c0xx00000x

www.rsc.org/xxxxxx

ARTICLE TYPE

A New Selective Chromogenic and Turn-On Fluorogenic Probe for Copper (II) in Solution and Vero Cells: Recognition of Sulphide by [CuL]

Ajit Kumar Mahapatra[*,†] Sanchita Mondal,[†] Saikat Kumar Manna,[†] Kalipada Maiti,[†] Rajkishor Maji,[†] Md. Raihan Uddin,[‡] Sukhendu Mandal,[‡] Deblina Sarkar,[§] Tapan Kumar Mondal[§] and Dilip Kumar Maiti[ʃ]

Received (in XXX, XXX) Xth XXXXXXXXX 20XX, Accepted Xth XXXXXXXXX 20XX
DOI: 10.1039/b000000x

A new coumarin-appended thioimidazole-linked imine conjugate, *viz*. **L** has been synthesized and characterized. The **L** has been found to recognize Cu^{2+} selectively among a wide range of biologically relevant metal ions. The chemosensing behavior of the **L** has been demonstrated through fluorescence, absorption, visual fluorescent color changes, ESI-MS and ^{1}H NMR titrations. The chemosensor **L** showed selectivity toward Cu^{2+} by switch on fluorescence among the 18 metal ions studied with a detection limit of 1.53 μM. The complex formed between **L** and Cu^{2+} is found to be 1:1 on the basis of absorption and fluorescence titrations and was confirmed by ESI-MS. DFT and TDDFT calculations were performed in order to demonstrate the structure of **L** and [**CuL**] and electronic properties of chemosensor **L** and their copper complex. This highly fluorescent [**CuL**] complex has been used to recognize sulphide selectively among the other allied anions. Microstructural features of **L** and its Cu^{2+} complex have been investigated by SEM imaging (scanning electron microscopy). The biological applications of **L** were evaluated in Vero cells and it was found to exhibit low cytotoxicity and good membrane permeability for the detection of Cu^{2+}.

Introduction

Copper is a essential trace element, the third most abundant (after Fe^{2+} and Zn^{2+}) in humans, and is present at low levels in a variety of cells and tissues with the highest concentrations in the liver,[1] and in the brain.[2] Copper is a redox-active nutrient that is needed at unusually high bodily levels for normal brain function.[3] Owing to the large oxygen capacity and oxidative metabolism of brain tissue, neurons and glia alike require copper for the basic respiratory and antioxidant enzymes cytochrome *c* coxidase (CcO) and Cu/Zn superoxide dismutase (SOD1), respectively. In addition, copper is a necessary cofactor for many brain-specific enzymes that control the homeostasis of neurotransmitters, neuropeptides, and dietary amines. However, it is toxic at higher concentration level, for example, the accumulation of Cu^{2+} in the liver and kidney may cause gastrointestinal, Wilson disease,[4] amyotrophic lateralsclerosis,[5] Menkes syndrome,[6] Alzheimer's disease,[7] hypoglycemia, dyslexia and infant liver damage.[8,9] Therefore, the development of molecular turn-on fluorescent probes for fast detection of Cu^{2+} in water or physiological samples is of toxicological and environmental concern.[10] However, fluorescence detection of Cu^{2+} by a turn-on response is particularly difficult due to its paramagnetic nature,[11] as unpaired electrons in close proximity to fluorescent dyes tend to quench emission. Therefore several ON-OFF fluorescent probes for Cu^{2+} have been reported.[12] Recently, many fluorescent chemosensors for Cu^{2+}- selective detection were reported and have been used with some success in biological applications.[13] However, some of them have shortcomings for practical application such as cross-sensitivities toward other metal cations, low water solubility, a narrow pH span, slow response, a low fluorescence quantum yield in aqueous media, and cytotoxicities of ligand. To prevent fluorescence quenching by Cu^{2+} and to achieve a practical "off-on" imaging with a strong fluorescent response upon binding the analyte, we devised a sensor system that separates the sensing and the signaling events. Two different fluorogenic ligands capable of metal chelation are employed whereby one of the ligands binds Cu^{2+}, while the other produces a fluorescent signal to report the binding event. Although the designed chemosensor is more effective in sensing Cu^{2+}, whereas other important cations such as Au^{3+}, Pd^{2+} and Zn^{2+} ions exhibited little bit fluorescence turn ON response.

Sulphide anion, as a toxic, hazardous and traditional pollutant, is widely spread in the environment. It is produced naturally and as a result of human activity. Natural sources include non-specific and anaerobic bacteria reduction of sulfates and sulfur containing

amino acids in meat proteins. Sulphide anion is found naturally in crude petroleum, volcanic eruption, and hot springs. It is released from stagnant or polluted waters and manure or coal pits. Sulphide anion may be produced by a variety of commercial methods as a byproduct in industrial processes, for example, conversion into sulfur and sulfuric acid, dyes and cosmetic manufacturing, production of an agricultural disinfectant, paper and wood pulp, etc.[14] Therefore, it is possible to bioconcentrate and biomagnify in the food-chain. So exposure to a high level of sulphide can lead to irritation in mucous membranes, unconsciousness, and respiratory paralysis.[15] Once sulphide anion is protonated, it becomes even more toxic. Therefore, the detection of sulphide anion has become very important from an industrial, environmental, and biological point of view.[16] A variety of detection techniques have been developed for the determination of sulphide anion,[17] Among them, sulphide anion sensing by fluorescence spectrometry has received much importance due to its high sensitivity and easy detection.[18] However, the development of fluorescent sensors for anions in aqueous media is still a challenging task because of the strong hydration nature of anions, which weakens the interactions of the chemosensors with the target anions.[19] This could be avoided by using the metal displacement approach, which is based on the stability constant of the complex formed by metal-anion affinity is larger than that of the complex of metal and its chemosensor.[20] Sulphide is known to react with copper ions to make a very stable CuS form with a very low solubility product constant K_{sp} = 6.3×10^{-36} that of cyanide one (3.2×10^{-20}). Recently, Nagano and Zeng groups reported new approaches for the detection of sulphide in live biological systems through the development of Cu^{2+} complex for chemoselective sulphide-responsive fluorescent sensors.[21] Recently, we presented a displacement-based sensing method by using metal-based ensembles for other anion recognition or sensing.[22,23] From this idea, we have successfully developed an ensemble of fluorescence and colorimetric sulphide chemosensors based on the traditional Cu^{2+} chemosensors.

Results and discussion

The fluorescent chemosensor molecule (**L**) has been synthesized by going through two consecutive steps starting from 3-bromoacetylcoumarin (1) followed by the preparation of its thiazolylamine derivative (2) by condensation reaction with thiourea as shown in Scheme 1.[24]

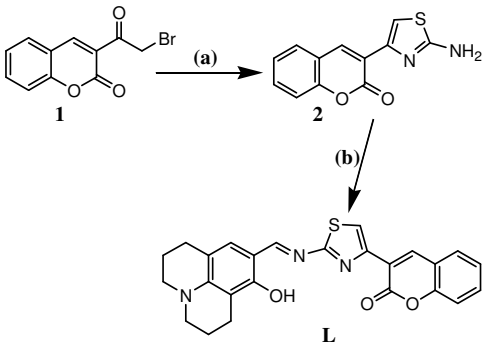

Scheme 1 Synthesis of **L**. Reagents and conditions: (a) thiourea, dry ethanol, reflux, 12 h; (b) 8-hydroxy-2,3,6,7-tetrahydro-1*H*,5*H*-benzo[ij]quinolizine-9-carboxaldehyde, dry ethanol, reflux, 6 h.

The final chemosensor molecule **L** has been synthesized by the condensation of 2 with 8-hydroxy-2,3,6,7-tetrahydro-1*H*,5*H*-benzo[ij]quinolizine-9-carboxaldehyde (b) in ethanolic medium with 72% yield (Scheme 1).[25] All the intermediates and the final chemosensor molecule were characterized by various analytical and spectral techniques. The structure of **L** was well characterized by ^{1}H NMR, ^{13}C NMR, and mass spectra (Fig. S3-S5, ESI†). The molecular structure of the intermediate thiazolylamine compound **2** has been established by ^{1}H NMR, ESI-MS as well as single-crystal XRD analysis (Fig. S1, S2 and S8, ESI†). Single crystals of 2 suitable for X-ray diffraction study were obtained by slow diffusion of methanol into the solution of 2 in chloroform and the data were collected[26] (Table S4, ESI†).

UV-vis and fluorescence spectral behavior of L. The sensitivity of **L** toward different metal ions and their preferential selectivity toward Cu^{2+} over the other ions has been studied by fluorescence and absorption titrations.

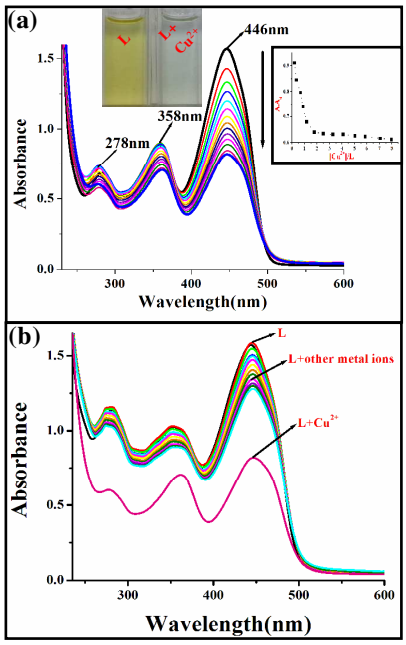

Fig. 1 (a) UV−vis absorption titration spectra of spectra of **L** (c = 4×10^{-5} M) in aq. CH_3CN (CH_3CN/H_2O = 7:3 v/v, 10 mM HEPES buffer, pH = 7.4) upon addition of Cu^{2+} (c = 2×10^{-4} M). Inset: The inset shows the relative absorption intensity (A/A_0) as a function of [Cu^{2+}]/[**L**], and the photographs showed the color change of **L** in the presence of Cu^{2+}. (b) Competitive absorption spectra of **L** in the presence of different metal ions (perchlorate, chloride, or nitrate salts of Hg^{2+}, Cd^{2+}, Fe^{2+}, Co^{2+}, Ni^{2+}, Mn^{2+}, Zn^{2+}, Au^{3+}, Cu^{2+}, Ag^{+}, Pd^{2+}, Cr^{3+}, Al^{3+}, Pb^{2+}, Ca^{2+}, Mg^{2+}, Na^{+}, and K^{+}) in aq. CH_3CN ($CH_3CN:H_2O$ = 7:3 v/v, 10 mM HEPES buffer, pH = 7.4).

The UV-vis absorption spectra of chemosensor **L** in aqueous acetonitrile ($CH_3CN:H_2O$ = 7:3 v/v, 10 mM HEPES buffer, pH = 7.4) are dominated by two absorption bands at 278 and 358 nm, respectively, and a low energy (LE) band centered at 446 nm

attributed to the iminothiazole moiety. During the titration, the concentration of **L** was kept constant at 40 μM and the mole ratio of Cu^{2+} was varied. The absorbance of 278, 358, and 446 nm bands is found to decrease upon addition of Cu^{2+} (Fig. 1a), indicating the interaction of Cu^{2+} with the iminothiazole/aromatic moiety. The low energy (LE) band at 446 nm was gradually decreases, upon addition of Cu^{2+} ions, which is responsible for the change of color from light yellow to colorless. This fact can be used for a 'naked-eye' detection of Cu^{2+} ions. However the absorption titration carried out with all the other metal ions showed no significant change, indicating their noninteractive nature with **L** (Fig. 1b). The binding affinities of Cu^{2+} toward **L** have also been calculated from the Benesi–Hildebrand equation using absorption data and found to have the association constants of 2.28×10^4 M^{-1}, respectively (Fig. S14A, ESI†).

The chemosensor **L** exhibits weak fluorescence emission at 500 nm owing to the isomerization of the imine C=N bond as well as excited-state intramolecular proton transfer (ESIPT) from the salicyl –OH to the imine nitrogen when excited at 446 nm in CH_3CN-H_2O mixture (7:3 v/v in 10 mM HEPES buffer at pH = 7.4) which has been well documented in literature pertaining to Schiff base molecular systems.[27-28]

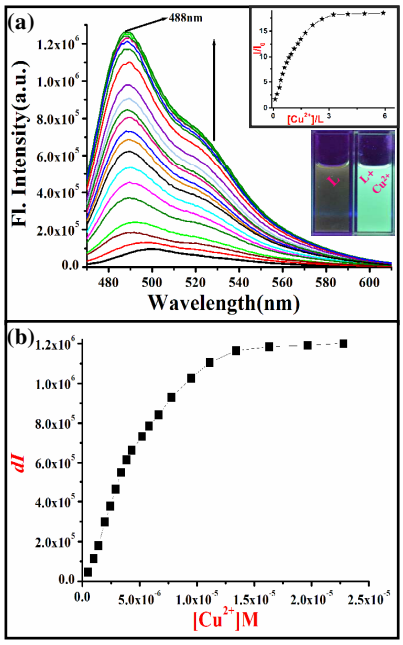

Fig. 2 (a) Fluorescence emission spectra obtained during the titration of **L** (c = 1×10^{-5} M) with Cu^{2+} (c = 1×10^{-4} M) in aqueous CH_3CN (CH_3CN:H_2O = 7:3 v/v, 10 mM HEPES buffer, pH = 7.4), λ_{ext} = 446 nm. Inset: The inset shows the relative fluorescence intensity (I/I_0) as a function of [Cu^{2+}]/[**L**] mole ratio, and fluorescence emission color changes of the receptor **L** solution on addition of Cu^{2+} ions. (b) Change of emission intensity at 500 nm with incremental addition of Cu^{2+} ions [λ_{ext} = 446nm].

Titration of **L** with Cu^{2+} results in the enhancement of the fluorescence intensity at 488 nm as a function of [Cu^{2+}] (Fig. 2a) and the intensity saturates at >1 equiv. In this connection, it is well known that Cu^{2+} is a paramagnetic ion with an unfilled d-shell and could strongly quench the emission of the fluorophore near it via electron or energy transfer. But in our case, the enhancement of emission of **L** after binding of Cu^{2+} ion is quite interesting and mentionable along with other few related existing systems.[29]

To our opinion, the *switch on* fluorescence emission is expected due to the chelation of Cu^{2+} through deprotonated phenolic oxygen, the imine and thiazole N atoms, and the lactone carbonyl oxygen. Such chelation leads to suppression of C=N bond isomerization to attain conjugated coplanar structure as well as ESIPT and fluorescence enhancement takes place as a consequence.[30] Further, chelation imparts rigidity to the system and the metal-fluorophore interaction is modulated, which are the underlying cause of chelation enhanced fluorescence (CHEF).[31]

A plot of the relative fluorescence intensity (I/I_0) vs [Cu^{2+}]/[**L**] mole ratio (Fig. 2a, inset) gives sigmoidal plot and exhibits midpoint ratio of 1:1 stoichiometric complex for **L** to Cu^{2+}. The binding affinities of Cu^{2+} toward **L** have been calculated from the Benesi- Hildebrand equation and found to have association constant 3.33×10^4 M^{-1} (Fig. S14B, ESI†).

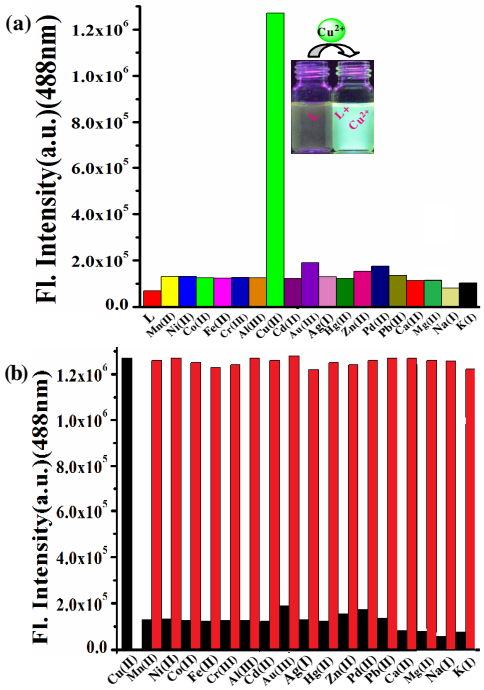

Fig. 3 (a) Histogram showing the relative fluorescence response of various metal ions (c = 1×10^{-4} M) with **L** (c = 1×10^{-5} M) in aq. CH_3CN (CH_3CN:H_2O = 7:3 v/v, 10 mM HEPES buffer, pH = 7.4), Inset: Fluorescence photograph of **L** and **L**+Cu^{2+}. (b) Fluorescence response of **L** (c = 1×10^{-5} M) to addition of 3 equiv. Cu^{2+} (c = 1×10^{-4} M) and 10 equiv. of other metal ions (c = 1×10^{-4} M) [the black bar portion] and to the mixture of 10 equiv. of other divalent metal ions with addition of 3 equiv. Cu^{2+} [the red bar portion].

The observed high K_a value clearly indicates the strong affinity of Cu^{2+} to **L**. Titration of **L** (500 nm) with 3 equiv. Cu^{2+} results in the sizable enhancement of fluorescence intensity at 488 nm as a function of the added Cu^{2+} concentration [($I_{complex}/I_{free\ ligand}$) ~ 18-

fold] (Fig. 2a). Under UV light, the solutions of **L** is weak fluorescent, whereas in the presence of Cu^{2+} an intense green color fluorescent was observed (Fig. 2a, inset) and no such fluorescent color was observed in case of the other metal ions (Fig. S13, ESI†). Thus, Cu^{2+} can easily be differentiated by its fluorescent color change from the other metal ions (Fig. S13, ESI†).

Further, the stoichiometry of the complex formed between **L** and Cu^{2+} has been derived to be 1:1 based on basis of a Job's plot (Fig. S9, ESI†). The formation of a 1:1 binding mode of the sensor with Cu^{2+} was also confirmed by the ESI-MS, where the spectrum obtained for the in situ complex results in a molecular ion peak at m/z = 524.7646 (calc. 524.09) (Fig. S6, ESI†). The mass spectrum is assignable to the mass of $[\mathbf{L}+Cu^{2+}+NH_4^+]^+$, supports the presence of copper. Therefore, we suggest that probe **L** coordinates with Cu^{2+} with 1:1 stoichiometry.

Competitive metal ion titrations. In order to check the practical utility of Cu^{2+} recognition by **L**, competitive titrations were carried out in the presence of other biologically and ecologically relevant metal ions. Fluorescence spectra (Fig. 3b) were recorded for the titration of **L** against Cu^{2+} in the presence of 10 equiv. of other different metal ions, viz. Au^{3+}, Ag^{+}, Hg^{2+}, Fe^{3+}, Pd^{2+}, Zn^{2+}, Cd^{2+}, Ni^{2+}, Co^{2+}, Mn^{2+}, Cr^{3+}, Al^{3+}, Pb^{2+}, Ca^{2+}, Mg^{2+}, Na^{+}, and K^{+}. In the fluorescence titration, the result found, none of these metal ions significantly affect the emission intensity of **L** upon the addition of Cu^{2+}, to have only marginal changes in the emission intensity, suggesting that none of these ions interfere in the fluorescence emission of the Cu^{2+} complex (Fig. 3b). Therefore, it can be concluded that **L** recognizes Cu^{2+} even in the presence of other metal ions. In the other fluorescence titrations were carried out in the same medium with 17 other different metal ions, viz. Au^{3+}, Ag^{+}, Hg^{2+}, Fe^{3+}, Pd^{2+}, Zn^{2+}, Cd^{2+}, Ni^{2+}, Co^{2+}, Mn^{2+}, Cr^{3+}, Al^{3+}, Pb^{2+}, Ca^{2+}, Mg^{2+}, Na^{+}, and K^{+}, found no significant fluorescence enhancement except Au^{3+}, Pd^{2+} and Zn^{2+} revealed relatively insignificant fluorescence ON responses in this region, manifesting the pronounced OFF–ON type of Cu^{2+} selectivity of **L** (Fig. 3a). Therefore, **L** is selective to Cu^{2+} among the 18 ions studied. Visual fluorescent color change experiments have been carried out to look at the behavior of **L** in the presence of various metal ions. The solution of **L** with > 1 equiv of Cu^{2+} ions converted the visual emission color change from faint yellow to bright green when excited with a hand-held 365 nm UV lamp, which is otherwise not present in case of the other metal ions studied (Fig. S13, ESI†). Therefore, Cu^{2+} can easily be differentiated by visual color change among the other metal ions.

The sensitivity of **L** for Cu^{2+} has been further evaluated by measuring the lowest concentration that can be determined. The fluorescence titration carried out between **L** and $[Cu^{2+}]$ by maintaining a 1:1 ratio gives a value of 1.53 μM suggesting its applicability to detect Cu^{2+} ions in aqueous medium at physiological conditions.

To be useful in biological applications, it is necessary for a fluorescent probe to operate over a suitable range of pH, especially at physiological pH. A series of buffers with pH values ranging from 1 to 13 was prepared by mixing sodium hydroxide solution and hydrochloric acid in HEPES buffer. Thus, we proceeded to investigate the effect of pH on the fluorescence intensity of the probe **L** in the absence or presence of Cu^{2+}. The results showed that fluorescence intensity (I_{488} nm) of **L** showed no apparent changes in the pH range from 6.0 to 9.0 no matter with or without Cu^{2+}, indicating that **L** is stable in this pH range and its response towards Cu^{2+} was also almost invariable in this pH range (Fig. S12, ESI†).

^{1}H NMR Titration Experiment. To know the mode of complexation of **L** with Cu^{2+}, we carried out ^{1}H NMR titration in $CDCl_3$. During the ^{1}H NMR titration of **L** with Cu^{2+}, the addition of 1 equiv. of Cu^{2+} into the solution of **L** in $CDCl_3$ provided the ^{1}H NMR spectrum to be very broad due to the complexation of paramagnetic Cu^{2+} to the **L**. The proton NMR signals corresponding to the thiazole (H_c) and imine proton (H_b) experiences considerable broadening owing to the binding of this region with paramagnetic Cu^{2+} (Fig. 4).

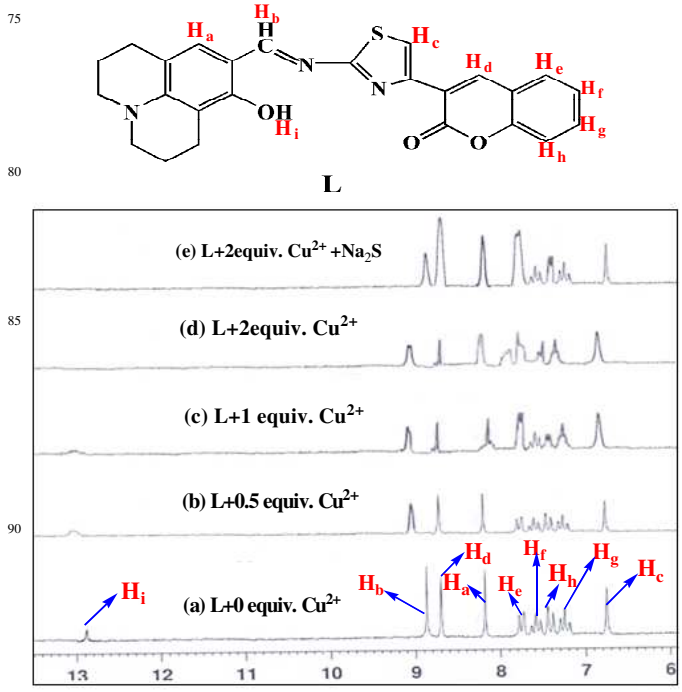

Fig. 4 Partial ^{1}H NMR spectra (400 MHz) of **L** in $CDCl_3$ at 25 °C and the corresponding changes after the gradual addition of different equivalents of copper perchlorate in MeOH- d_4 from (a) **L**, (b) **L** + 0.5 equiv. Cu^{2+}, (c) **L** + 1.0 equiv. Cu^{2+}, (d) **L** + 2.0 equiv. Cu^{2+} and (e) **L** + 2.0 equiv. Cu^{2+} + Na_2S.

However, treatment of the [**CuL**] system with sulphide ions afforded a well resolved spectrum, which was almost identical with the ^{1}H NMR spectrum of **L** itself (Fig. S3, ESI†). To further clarify the spectrum, the product of $[\mathbf{CuL}+S^{2-}]$ was isolated by a silica gel column and was then subjected to ^{1}H NMR analysis. The ^{1}H NMR of the resulting product is essentially identical to that of free **L**.

Density Functional Theory (DFT) Calculations. To verify the configuration of [**CuL**] and to investigate the electronic structure

and the electronic transitions of the π-conjugated copper complex, DFT geometry optimizations followed by TD-DFT calculations at the B3LYP level[32] were carried out. All element except Cu were assigned 6-31+G(d) basis set. The LANL2DZ basis set with effective core potential (ECP) set of Hay and Wadt [4] was used for Cu. The optimized geometries of **L** and [**CuL**] complex are shown in (Fig. 5) the complex shows that the Cu^{2+} ion binds to **L** very well through four coordination sites, and the whole molecular system forms a nearly planar structure.

The geometry optimizations for **L** and [**CuL**] complex were done in a cascade fashion starting from semiempirical PM2 followed by *ab initio* HF to DFT B3LYP by using various basis sets, *viz*., PM2 → HF/STO-3G → HF/3-21G → HF/ 6-31G → B3LYP/ 6-31G(*d,p*). For [**CuL**] complex, a starting model was generated by taking the DFT optimized **L** and placing the Cu^{2+} ion well in the core of the coumarin lactonecarbonyl O, enamine N, phenolic OH and / thiazole N as donors moieties at a non-interacting distance. This model was then optimized initially using HF/3-21G level of calculations, and the output structure from this was taken as input for DFT calculations performed using B3LYP with LANL2DZ relativistic pseudopotentials basis set for Cu^{2+} and 6-31+G(*d*,*p*) for all other atoms in the complex.

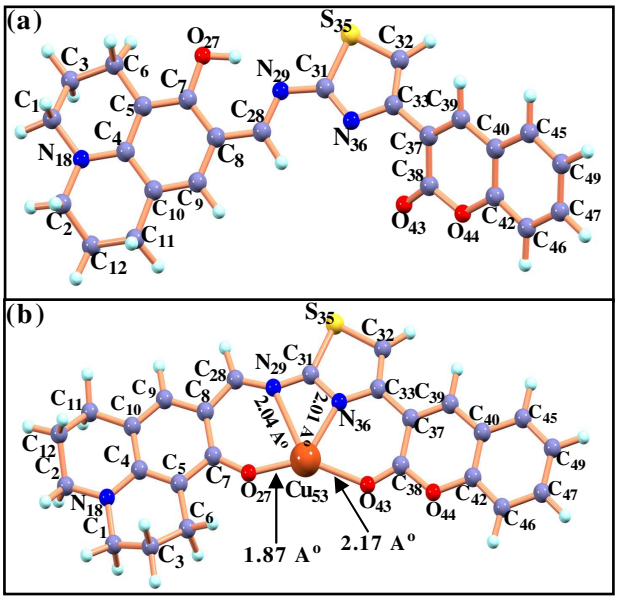

Fig. 5 B3LYP Optimized structure of (a) **L** by DFT/B3LYP/6-31+G(d) method (b) **L**-Cu^{2+} complex by DFT/UB3LYP method.

The geometry optimization resulted in the conformational changes at the two sides of thioimidazole ring *i.e*.; coumarin and aminophenol parts to accommodate copper ion. The conformational changes can be estimated through the torsional angles of the two sides (Table S1, ESI†) and the structure given in (Fig. 5). In the progress, the lactone oxygen of the coumarin moiety and phenolate oxygen of the amiophenol part turned to the same direction form a binding core. In the **CuL** optimized structure, the copper is bound by the two nitrogen atoms (imine and thioimidazole) and two oxygen atoms (coumarin lactone and phenolate oxygens) in the binding core (N_2O_2) leads to highly distorted geometries about the copper centers that deviate from both the tetrahedral as well as that of the square planar.

The optimized complex of Cu^{2+} with **L** associated with four bonds (N_{29}–Cu, N_{36}–Cu, O_{43}–Cu and O_{27}–Cu) to the central ion with their distances of 2.04, 2.01, 2.17 and 1.87 Å respectively (Table S1, ESI†).[33] The geometry about Cu^{2+} is significantly distorted by exhibiting coordination angles in the range 65.59–120.97^0. The spatial distributions and orbital energies of HOMO and LUMO of **L** and [**CuL**] were also determined (Fig. 6a).

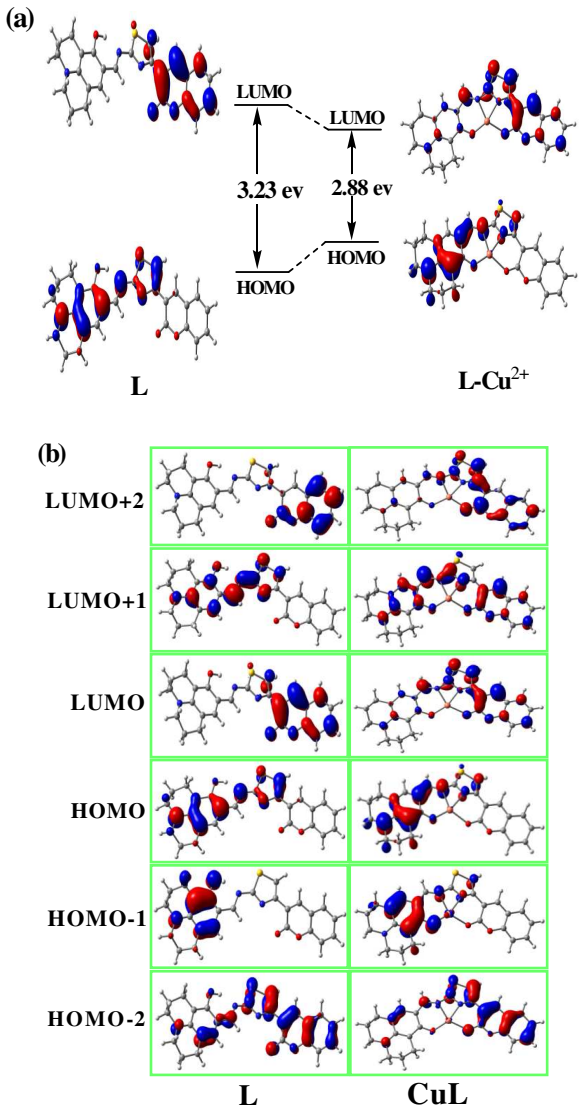

Fig. 6 (a) HOMO and LUMO distributions of **L** and **L**–Cu^{2+} complex. (b) Molecular orbital plots of **L** and **L**–Cu^{2+}.

The π electrons on the relevant HOMOs and LUMOs of [**CuL**] complex are essentially distributed in the entire coumarinthioimidazole–aminophenol backbone. By contrast, in the case of **L**, the π electrons on HOMO and HOMO–1 are primarily resided on the electron-donating aminophenol moiety, whereas those on LUMO, HOMO–2 and LUMO +2 are mainly located on the electron withdrawing coumarin moiety (Fig. 6b).

This indicates that **L** bears efficient electron transfer from the aminophenol moiety to the coumarin parts, thus rendering the fluorescence relatively weak (ϕ = 0.020). By contrast, the nearly complete overlap of electrons on the transition orbitals may induce the strong fluorescence emission for [**CuL**] complex (ϕ = 0.62).[34] Moreover, the HOMO–LUMO energy gap of complex become much smaller relative to that of probe **L**. The energy gaps between HOMO and LUMO in the probe **L** and [**CuL**] complex were 3.23 eV and 2.88 eV respectively (Fig. 6a).

SEM imaging studies. To understand the aggregation property of the **L** and [**CuL**], and its effect on their chemo-sensing property, scanning electron microscope (SEM) imaging were carried out. The **L** and [**CuL**] are possessing charge transfer, hydrogen bonding, π- π stacking, van der Waals force of attraction which enforce the compounds to form sheet-like 2D nanostructure and globular material respectively (Fig. 7a and b). Exact mechanism aggregation to construct uniform globular material is unknown to us. However, in presence of Cu^{2+}-ion a strong complexation with the ligand along with charge transfer is expected. This SEM imaging study supports the unprecedented chemosensing nature of **L** and [**CuL**] which can be utilized for cell imaging.

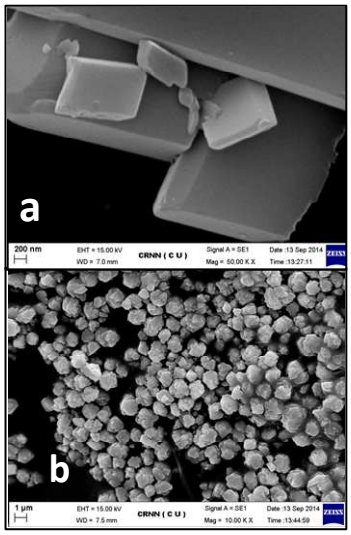

Fig. 7 (a) Monolayer SEM image of **L** and (b) SEM image of **L**–Cu^{2+} complex.

Fluorescence and UV-Vis spectroscopic studies of [CuL] complex in presence of S^{2-}. Since **L** detects Cu^{2+} selectively, the in situ prepared [**CuL**] complex has been used for its anion recognition studies. Owing to the strong affinity of Cu^{2+} towards sulphide the highly fluorescent [**CuL**] complex has been studied for their secondary sensing property toward selective anion.[35] The chemosensing ensemble was prepared in situ by mixing **L** and Cu^{2+} in 1:1 ratio and it have been used for the anion recognition studies by different anions, viz., F^-, Br^-, S^{2-}, I^-, CN^-, SO_4^{2-}, SCN^-, AcO^-, Cl^-, $H_2PO_4^-$, PO_4^{3-}, NO_3^-, ClO_4^- and HSO_4^-. All the anion titrations exhibited no significant change in the fluorescence intensity except sulphide and cyanide.

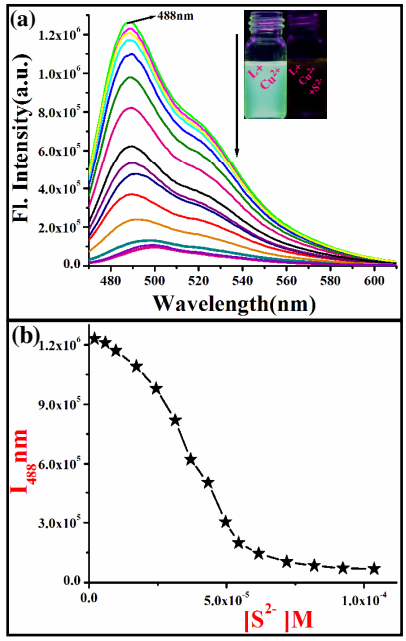

Fig. 8 (a) Fluorescence spectra of **L** (c = 1×10^{-5} M) with 3 equiv. of Cu^{2+} upon addition of sodium sulphide (c = 4×10^{-4} M) in aq CH_3CN ($CH_3CN:H_2O$ = 7:3 v/v, 10 mM HEPES buffer, pH = 7.4) and Photographs of **L**+Cu^{2+}, **L**+Cu^{2+}+S^{2-} in color changes. (b) Fluorescence intensity (I) vs [S^{2-}] mole ratio plot at 488 nm, [λ_{ext} = 446nm].

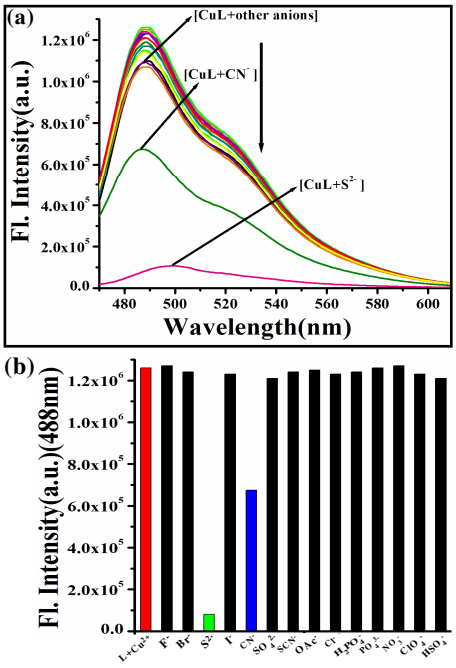

Fig. 9 (a) Competitive fluorescence spectra of **CuL** (1.0×10^{-5} M) in the presence of tetrabutyl ammonium salt of different anions (4.0×10^{-4} M) (F^-, Br^-, S^{2-}, I^-, CN^-, SO_4^{2-}, SCN^-, AcO^-, Cl^-, $H_2PO_4^-$, PO_4^{3-}, NO_3^-, ClO_4^- and HSO_4^-.) in CH_3CN-H_2O(7:3 v/v, pH = 7.4). (b) The anion sensitivity profile for **CuL**: the change in the emission intensity of **CuL** (1.0×10^{-5} M) in presence of 4.5 equivalents of S^{2-} ion, and 10 equivalents of other interfering anions in aq. CH_3CN ($CH_3CN:H_2O$=7:3 v/v, 10 mM HEPES buffer, pH = 7.4).

During the titration of [**CuL**] with sulphide, the emission band observed at 488 nm is quenched (Fig. 8a) gradually to reach an intensity that is similar to that of **L**. This is exactly reverse to what happens when **L** is titrated with Cu^{2+}, indicating the removal of Cu^{2+} by sulphide and thereby the releasing the free **L**. This is true even with cyanide (Fig. S16, ESI†).

Thus the [**CuL**] complex acts as a secondary recognition ensemble toward sulphide, and cyanide. The minimum concentration of sulphide that can be detected by [**CuL**] has been found to be 11.4 μM (Fig. S15B, ESI†).

In order to support the results obtained from the fluorescence studies, the removal of Cu^{2+} by sulphide ion, similar absorption titrations were carried out. During the titration of the [**CuL**] by CN^- (Fig. 10a), the low energy absorption band arising from the precursor complex observed at 446 nm have been progressively increases and gradual addition of sulphide two bands, one at 278 nm and the other at 358 nm, which correspond to the free receptor **L**, and the absorbance of these bands increases (Fig. 10a).

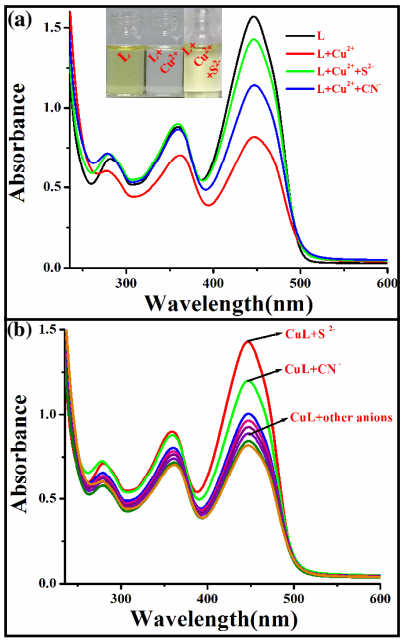

Fig. 10 (a) Changes in the absorption spectra of **L**–Cu complex (1.0×10^{-5} M) in presence of S^{2-}, CN^- (4.0×10^{-4} M) in aq. CH_3CN ($CH_3CN:H_2O$ = 7:3 v/v, 10 mM HEPES buffer, pH = 7.4). (b) Competitive UV–vis titration spectra of **CuL** (1.0×10^{-5} M) in the presence of tetrabutyl ammonium salt of different anions (4.0×10^{-4} M) (F^-, Br^-, S^{2-}, I^-, CN^-, SO_4^{2-}, SCN^-, AcO^-, Cl^-, $H_2PO_4^-$, PO_4^{3-}, NO_3^-, ClO_4^- and HSO_4^-.) in CH_3CN-H_2O(7:3 V/V, pH = 7.4).

All this suggests the disruption of the [**CuL**] complex followed by the removal of Cu^{2+} by the sulphide as well as cyanide ions to result in free receptor, it has been noted that the changes observed for different bands during the titration between the [**CuL**] and S^{2-} is exactly reverse to that observed during the titration of **L** with Cu^{2+} (Fig. 1a). This suggests a displacement mechanism during the titration of S^{2-}. Similar observations were noticed with CN^-. Sulphide selective signaling was not affected by the presence of other common interfering anions. Competition experiments of the [**CuL**] system revealed that the S^{2-} induced fluorescence turn-off was retained in the presence of 100 equiv. of other common, coexisting anions. Thus, the ensemble seems to be useful for selectively sensing S^{2-} even involving relevant anions.

Reusability and Reversibility of the Receptor L. The reversibility is an important aspect of any receptor to be employed as a chemical sensor for detection of specific metal ions. To examine whether the process is reversible, an excess amount of S^{2-} was added into the solution of [**CuL**] ensemble.

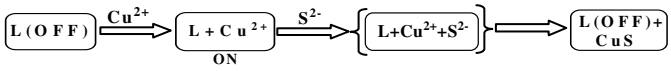

Scheme 2 Schematic Presentation for Fluorescence Quenching.

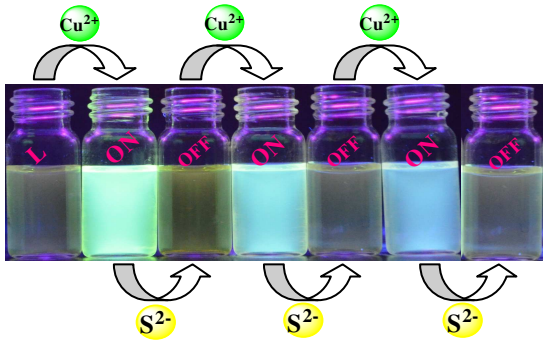

Fig. 11 Fluorescence experiment showing on-off reversible visual fluorescent color changes after each addition of Cu^{2+} and S^{2-} sequentially.

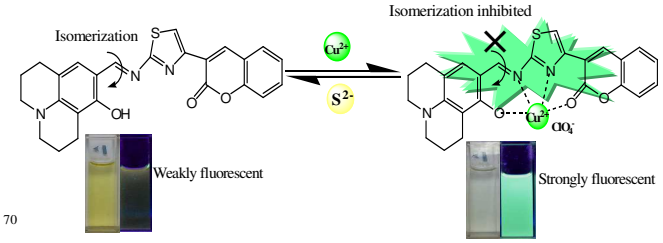

Scheme 3 Proposed mechanism for the fluorescence changes of **L** upon addition of Cu^{2+}.

The bright green fluorescence immediately turned off (Fig. 8a, inset). The reusability of [**CuL**] in sensing S^{2-} has been demonstrated by carrying out four alternate cycles of titration of [**CuL**] with S^{2-} followed by Cu^{2+}. Titration of [**CuL**] with S^{2-} shows significant switch off fluorescence, and the fluorescence is regained when Cu^{2+} is added to result in the switch on mode. Three such consecutive cycles are shown in Fig. 11, and the results clearly demonstrate the reversible property of **L** in sensing Cu^{2+} followed by S^{2-} / CN^- (Fig. S16, ESI†).

Detection and imaging in living cells. The desirable features of chemosensor **L** such as high sensitivity with a turn-on fluorescence, fast response, reversibility, working well at physiological pH, and high selectivity encouraged us to further evaluate the potential of the sensor for imaging Cu^{2+} in living

cells. Here Vero cells (very thin endothelial cell) were used as models (Experimental section). Before microscopic imaging, all the solutions were aspirated and mounted on slides in a mounting medium containing DAPI (1 μg /mL) to label the cell nuclei and stored in dark before microscopic images are acquired. The Vero cells incubated with only sensor **L** (1 μM) exhibited very weak intracellular fluorescence. Again, the cells were pre-treated with Cu^{2+} in the growth medium for 30 min. The cells were then washed with PBS to remove the remaining Cu^{2+} and further incubated with probe **L** for 30 min.

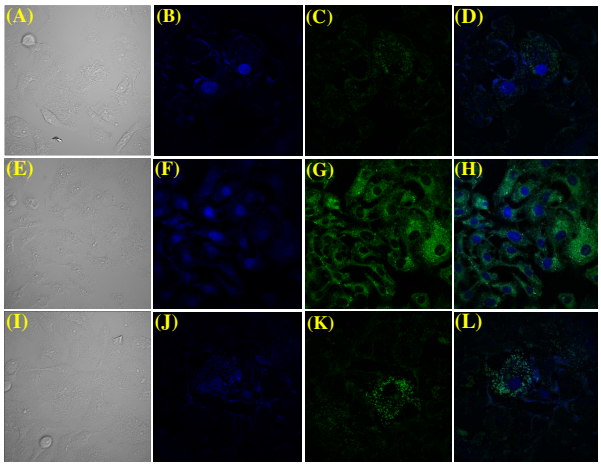

Fig. 12 Confocal microscopic images of probe in Vero 76 cells pretreated with Cu^{2+}: (A) bright field image of the cells of controlled set. (B) only Cu^{2+} at 1.0×10^{-4} M concentration, nuclei counterstained with DAPI (1 μg/mL). (C) only Cu^{2+} at 1.0×10^{-4} M concentration. (D) overlay of (B and C). (E) bright field image of the cells stained with probe **L** at concentration 1.0×10^{-6} M. (F) image scan of DAPI for E. (G) with probe **L** at concentration 1.0×10^{-6} M detected on λ_{ext} = 450 nm, λ_{em} = 519 nm. (H) overlaid image of F and G. (I) bright field image of the cells treated with 1.0×10^{-4} M Cu^{2+}, 1.0×10^{-6} M probe **L** and Na_2S at concentration 4.0×10^{-5} M (J) cells of I scanned for DAPI (K) cells of I scanned at λ_{ext} = 473, λ_{em} = 519 (L) overlay of J and K. All images were acquired with a 60x objective lens. Scale bar represents 20 μm.

Vero cells incubated with chemosensor **L** exhibited very weak fluorescence, whereas a bright green fluorescence signal was observed in the cells stained with both the chemosensor **L** and Cu^{2+}, which in good agreement with the fluorescence turn-on profile of the sensor in the presence of Cu^{2+} in the solution (Fig. 12[E-H]). Moreover, bright green colored fluorescence cells obtained from the incubation of the receptor **L** followed by treatment with Cu^{2+} became invisible in fluorescence upon addition of Na_2S (40 μM) (Fig. 12[I-L]). The results establish that sensor **L** is cell membrane permeable and capable of sensing Cu^{2+} in living cells. To the best of our knowledge, this is the first known thiazole-coumarin-based conjugate in the literature which has been demonstrated to recognize Cu^{2+} in live cells. Cells were intact and showed healthy spread and adherent morphology during and after the labeling process with chemosensor **L**, indicating an absence of cytotoxic effects.

Conclusion

The iminothioimidazole-phenolic-coumarin based probe **L** was synthesized and characterized. The probe **L** was found to be sensitive and selective fluoroionophore of Cu^{2+} among the eighteen different metal ions studied in HEPES buffer medium. The selectivity and sensitivity were demonstrated on the basis of fluorescence, absorption, and ^{1}H NMR spectroscopy, ESI mass spectrometry, and visual fluorescent color changes. Interaction of Cu^{2+} with **L** enhances the fluorescence emission and induces a turn on response in electronic and fluorescence spectra in the visible region. Thus, these receptors could be used as a dual probe for visual detection through change in color and fluorescence. Fluorescence and absorption spectroscopy provides information for the formation of a 1:1 complex between Cu^{2+} and **L**, and ESI-MS confirms the fact. The association constant, K_a for **L** with Cu^{2+} is in the order of 10^4 M^{-1} based on fluorescence as well as absorption studies, suggesting a strong binding for Cu^{2+}. The receptor **L** has been shown to be sensitive with a minimum detection limit of 1.53 μM ± 0.1 ppm Cu^{2+}. The Cu^{2+} binding characteristics of **L** has been studied by computational calculations at DFT level and TDDFT calculations were carried out to demonstrate the electronic properties of **L** and the corresponding copper complex. The in situ prepared copper complex of **L**, *viz*., **L**–Cu, was able to detect S^{2-} exactly reverse manner to what happens when Cu^{2+} is added to **L** in fluorescence spectroscopy. To know the supramolecular microstructural features of **L** and **L**–Cu complex, SEM studies were carried out in which the spherically shaped particles of **L** were found enlarged as well as aggregated in the complex. Nonfluorescent images were observed when Vero cells were incubated with probe **L** alone. However, strong green fluorescence was observed in Vero cells in the presence of Cu^{2+}. Hence, these results clearly indicate that the probe **L** is effective intracellular Cu^{2+} imaging agents with cell permeability.

Experimental Section

General Information and Materials. All the solvents were of analytic grade. All cationic compounds such as perchlorate of Hg^{2+}, Cd^{2+}, Fe^{2+}, Co^{2+}, Ni^{2+}, Mn^{2+}, Zn^{2+}, Au^{3+}, $Cu(ClO_4)_2$, nitrate of Ag^+, Pb^{2+}, chlorides of Cr^{3+}, Al^{3+}, and Pb^{2+}, were purchased from Sigma–Aldrich Chemical Co., stored in a desiccators under vacuum containing self-indicating silica, and used without any further purification. Solvents were dried according to standard procedures. Unless stated otherwise, commercial grade chemicals were used without further purification. Elix Millipore water was used throughout all experiments. All reactions were magnetically stirred and monitored by thin-layer chromatography (TLC) using Spectrochem GF254 silica gel coated plates. Column chromatography was performed with activated neutral aluminum oxide. FTIR spectra were recorded as KBr pellets using a JASCO FTIR spectrometer (model FTIR-460 plus). The ^{1}H NMR spectra were recorded on Bruker 400 MHz spectrometer. Mass spectra were carried out using a Waters QTOF Micro YA 263 mass spectrometer. The ^{1}H NMR chemical shift values are expressed in ppm (δ) relative to $CHCl_3$ (δ = 7.26 ppm). UV–vis and

fluorescence spectra measurements were performed on a JASCO V530 and a Photon Technology International (PTI-LPS-220B) spectrofluorimeter, respectively. The following abbreviations are used to describe spin multiplicities in ^{1}H NMR spectra: s = singlet; d = doublet; t = triplet; m = multiplet.

Synthesis and Characterization of L: Synthesis of (2): A mixture of compound 1 (3-bromoacetyl coumarin) (0.50 g, 1.87 mmol) and thiourea (0.168 g, 2.21 mmol) in 15ml absolute ethanol was refluxed for 12 h. After the completion of the reaction (monitored by TLC) the solvent was evaporated and the reaction mixture was poured into ice-water, and powdered product was extracted with $CHCl_3$. The organic layer was washed with saturated aqueous solution of NaCl, dried over anhydrous $MgSO_4$ and evaporated to give a yellow solid which was crystallized from MeOH/$CHCl_3$ (1:1) solution to give compound 2 in 69% yield; M.P. > 250˚C. ^{1}H NMR (400 MHz, d_6-DMSO, $Si(CH_3)_4$, J (Hz), δ (ppm)): 8.50 (1H, s), 7.83(1H, d, J=7.76 Hz), 7.60 (1H, t, J=7.82 Hz), 7.50 (1H, s), 7.43 (1H, d, J=8.28 Hz), 7.37 (1H, t, J=7.52 Hz), 7.16 (2H, s). TOF MS ES$^+$, m/z = 245.0093, $[M+H]^+$, calc. for $C_{12}H_8N_2O_2S$ =244.26.

Synthesis of chemosensor L. To a mixture of compound 2 (0.112g, 0.4608mmol) and 2,3,6,7-tetrahydro-1H,5H-benzo[ij]quinolizine-9-carboxaldehyde (3) (0.10g, 0.4608mmol) in dry EtOH (10ml) 2-3 drops of AcOH was added; then the reaction mixture was refluxed for 4-6 hours. After the completion of the reaction the solvent was evaporated and the deep yellow solid precipiteted was filtered through suction, washed with milipore water and thereafter washed several times with EtOH and dried in air. The deep yellow compound **L** was collected in 72% yield; M.P. > 250˚C. ^{1}H NMR ($CDCl_3$, 400 MHz) δ (ppm): 12.91 (1H, s, -OH), 8.84 (1H, s, -CH=N), 8.72 (1H, s), 8.20 (1H, s), 7.63 (1H, d, J = 6.8 Hz), 7.52 (1H, t, J=7.2 Hz) , 7.36 (1H, d, J=8.2 Hz), 7.30 (1H, t, J=7.7 Hz), 6.85 (1H, s), 3.31-3.26 (4H, q, J=8Hz), 2.75-2.68 (4H, m), 1.95 (4H, t, J=5.6). ^{13}C NMR ($CDCl_3$, 500 MHz) δ (ppm): 19.2, 19.9, 20.9, 21.8, 26.4, 31.1, 33.0, 49.1, 49.4, 105.2, 107.0, 113.2, 113.3, 115.5, 116.1, 118.8, 120.2, 123.7, 127.5, 130.5, 138.4, 144.7, 147.7, 152.1, 162.2; LCMS ES+, m/z = 444.2, $[M+H]^+$, calcd for $C_{25}H_{21}N_3O_3S$ = 443.13.

UV−Vis Spectral Studies. A stock solution of the probe **L** (4.0×10^{-5} M) was prepared in CH_3CN/H_2O (7:3 v/ v). Solutions of 2.0×10^{-4} M salts of the respective cation were prepared in Millipore water. All experiments were carried out in CH_3CN/H_2O solution (CH_3CN/H_2O = 7:3 v/v, 10 mM HEPES buffer, pH = 7.4). In titration experiments, each time a 4×10^{-5} M solution of **L** was filled in a quartz optical cell of 1 cm optical path length, and the ion stock solutions were added into the quartz optical cell gradually by using a micropipette. Spectral data were recorded at 1 min after the addition of the ions. In selectivity experiments, the test samples were prepared by placing appropriate amounts of the anions/cations stock into 2 mL of solution of **L** (4×10^{-5} M).

Fluorescence Spectral Studies. A stock solution of the probe **L** (1.0×10^{-5} M) was prepared in CH_3CN/H_2O (7:3 v/ v). Solutions of 1.0×10^{-4} M salts of the respective cation were prepared in Millipore water. All experiments were carried out in CH_3CN/H_2O solution (CH_3CN/H_2O = 7:3 v/v, 10 mM HEPES buffer, pH = 7.4). In titration experiments, each time a 1×10^{-5} M solution of **L** was filled in a quartz optical cell of 1 cm optical path length, and the ion stock solutions were added into the quartz optical cell gradually by using a micropipet. Spectral data were recorded at 1 min after the addition of the ions. In selectivity experiments, the test samples were prepared by placing appropriate amounts of the anions/cations stock into 2 mL of solution of **L** (1×10^{-5} M). For fluorescence measurements, excitation was provided at 446 nm, and emission was collected from 470 to 610 nm.

Finding the Detection Limit. The detection limit was calculated on the basis of the fluorescence titration (Figure S13, Supporting Information). The fluorescence emission spectrum of **L** was measured 10 times, and the standard deviation of blank measurement was achieved. To gain the slope, the ratio of the fluorescence intensity at 488 nm was plotted as a concentration of Cu^{2+}. So the detection limit was calculated with the following equation.

$$\text{Detection limit} = 3Sb1/S \qquad (1)$$

where Sbl is the standard deviation of blank measurement and S is the slope of the calibration curve.

Computational Studies. All geometries for **L** and **L**-Cu^{2+} were optimized by density functional theory (DFT) calculations were performed with Gaussian09 program package,[36] with the aid of the GaussView visualization program.

Cell Line and Cell Culture. Vero cell (very thin endothelial cell) (Vero 76, ATCC No CRL-1587) lines were prepared from continuous culture in Dulbecco's modified Eagle's medium (DMEM, Sigma Chemical Co., St. Louis, MO) supplemented with 10% fetal bovine serum (Invitrogen), penicillin (100 µg/mL), and streptomycin (100 µg/mL). The Vero 76 were obtained from the American Type Culture Collection (Rockville, MD) and maintained in DMEM containing 10% (v/v) fetal bovine serum and antibiotics in a CO_2 incubator. Cells were initially propagated in 75 cm^2 polystyrene, filter-capped tissue culture flask in an atmosphere of 5% CO_2 and 95% air at 37°C in CO_2 incubator. When the cells reached the logarithmic phase, the cell density was adjusted to 1.0×10^5 per/well in culture media. The cells were then used to inoculate in a glass bottom dish, with 1.0 mL (1.0×10^4 cells) of cell suspension in each dish. After cell adhesion, culture medium was removed. The cell layer was rinsed twice with phosphate buffered saline (PBS), and then treated according to the experimental need.

Cell Imaging Study. For confocal imaging studies Vero cells, 1×10^4 cells in 1000 µL of medium, were seeded on sterile 35 mm covered Petridis, glass bottom culture dish (ibidi GmbH, Germany), and incubated at 37°C in a CO_2 incubator for 10 hours. Then cells were washed with 500 µL DMEM followed by incubation with 1.0 x 10^{-4} M $Cu(ClO_4)_2$ dissolved in 500 µL DMEM at 37°C for 1 h in a CO_2 incubator and observed under an

Olympus IX81 microscope equipped with a FV1000 confocal system using 1003 oil immersion Plan Apo (N.A. 1.45) objectives. Images obtained through section scanning were analyzed by Olympus Fluoview (version 3.1a; Tokyo, Japan) with excitation at 446 nm monochromatic laser beam, and emission spectra were integrated over the range 470-600 nm (single channel). The cells were again washed thrice with phosphate buffered saline PBS (pH 7.4) to remove any free $Cu(ClO_4)_2$ and incubated in PBS containing probe **L** to a final concentrations of 1.0 x 10^{-6} M, incubated for 10 min followed by washing with PBS three times to remove excess probe outside the cells and images were captured. In a separate culture dish undergoing the same treatment the cells were then treated with 4.0×10^{-5} M of Na_2S solution for 1 h; the cells were washed with PBS three times to remove free compound and ions before analysis. In separate culture dish the cells were similarly treated with 1.0×10^{-6} M probe **L**, incubated for 10 min, washed thrice with PBS and the image was captured to get any possible background fluorescence. According to the need of the experiment we follow similar procedures to label the cell nuclei by treatment with DAPI (1 μg/mL) followed by three times wash with PBS and subsequently image was captured with excitation wavelength of laser was 473 nm, and emission was 519 nm. For all images, the confocal microscope settings, such as transmission density, and scan speed, were held constant to compare the relative intensity of intracellular fluorescence. Before microscopic imaging, all the solutions were aspirated and mounted on slides in a mounting medium containing DAPI (1 μg /mL) to label the cell nuclei and stored in dark before microscopic images are acquired.

Cytotoxicity Assay. The cytotoxic effects of probe **L**, $Cu(ClO_4)_2$, and **L**─Cu^{2+}complex were determined by an MTT [3-(4,5-dimethylthiazol-2-yl)-2,5-diphenyltetrazolium bromide] assay following the manufacturer's instruction (MTT 2003, Sigma-Aldrich, MO). Vero cells were cultured into 96-well plates (10^4 cells per well) for 24 h. After overnight incubation, the medium was removed, and various concentrations of **L**, $Cu(ClO_4)_2$, and **L**─Cu^{2+} complex (0, 5, 25, 50, 75, and 100 μM) made in DMEM were added to the cells and incubated for 24 h. Control experiments were set with DMSO, cells without any treatment and cell-free medium were also included in the study. Following incubation, the growth medium was removed, and fresh DMEM containing MTT solution was added. The plate was incubated for 3–4 h at 37°C. Subsequently, the supernatant was removed, the insoluble colored formazan product was solubilized in DMSO, and its absorbance was measured in a microplate reader (Perkin-Elmer) at 570 nm. The assay was performed in triplicate for each concentration of **L**, $Cu(ClO_4)_2$, and **L**─Cu^{2+}. The OD value of wells containing only DMEM medium was subtracted from all readings to get rid of the background influence. The cell viability was calculated by the following formula: (mean OD in treated wells / mean OD in control wells) x 100.

Acknowledgment

We thank the DST-West Bengal [Project no. 124(Sanc.)/ST/P/S&T/9G-17/2012] for financial support. SM and SKM thanks to the UGC, New Delhi for a fellowship.

Notes and references

†Department of Chemistry, Indian Institute of Engineering Science and Technology, Shibpur, Howrah – 711103, India.

‡ Department of Microbiology, Ballygunge Science College, Kolkata-700019.

§Department of Chemistry, Jadavpur University, Kolkata-700032, India.

ʃ Department of Chemistry, University of Calcutta, Kolkata-700009, India.

* Corresponding author: Email: akmahapatra@rediffmail.com, Fax: +913326684564

† Electronic Supplementary Information (ESI) available: [details of any supplementary information available should be included here]. See DOI: 10.1039/b000000x/.

1 A. Mathie, G. L. Sutton, C. E. Clarke and E. L. Veale, *Pharm. Ther.*, 2006, **111**, 567.

2 J. Sto¨ckel, J. Safar, A. C. Wallace, F. E. Cohen and S. B. Prusiner, *Biochem*., 1998, 37, 7185.

3 (a) B. Halliwell and J. M. C. Gutteridge, *Biochem. J*., 1984, **219**, 1.

4 P. C. Bull, G. R. Thomas, J. M. Rommens, J. R. Forbes and D. W. Cox, *Nat. Genet*., 1993, **5**, 327.

5 J. S. Valentine and P. J. Hart, *Proc. Natl. Acad. Sci. U.S.A*., 2003, **100**, 3617.

6 C. Vulpe, B. Levinson, S. Whitney, S. Packman and J. Gitschier, *Nat. Genet*., 1993, **3**, 7.

7 Y. H. Hung, A. I. Bush and R. A. Cherny, *J. Biol. Inorg. Chem*., 2010, **15**, 61.

8 M. C. Linder and M. Hazegh-Azam, *Am. J. Clim. Nutr*., 1996, **63**, 797S.

9 R. Uauy, M. Olivares and M. Gonzalez, *Am. J. Clim. Nutr*., 1998, **67**, 952S.

10 (a) M. Y. Pamukoglu and F. Kargi, *J. Hazard. Mater*., 2007, **148**, 2744; (b) P. G. Welsha, J. Lipton, C. A. Mebane and J. C. A. Marr, *Ecotoxicol. Environ. Saf*., 2008, **69**, 199; (c) K. N. Buck, J. R. M. Ross, A. R. Flegal and K. W. Bruland, *Environ. Res*., 2007, **105**, 5; (d) E. Van Genderen, R. Gensemer, C. Smith, R. Santore and A. Ryan, *Aquat. Toxicol*., 2007, **84**, 279; (e) P. Kumar, R. K. Tewari and P. N. Sharma, *Plant Cell Rep*., 2008, **27**, 399.

11 A. P. de Silva, H. Q. N. Gunarante, T. Gunnlaugsson, A. J. M. Huxley, C. P. McCoy, J. T. Rademacher and T. E. Rice, *Chem. Rev*., 1997, **97**, 1515.

12 (a) Q. Zeng, P. Cai, Z. Li, J. Qin and B. Z. Tang, *Chem. Commun*., 2008, 1094; (b) J. Xie, M. Me´nand, S. Maisonneuve and R. Me´tivier, *J. Org. Chem*., 2007, **72**, 5980; (c) S. M. Park, M. H. Kim, J.-I. Choe, K. T. No and S.-K. Chang, *J. Org. Chem*., 2007, **72**, 3550; (d) Z. Guo, W. Zhu, L. Shen and H. Tian, *Angew. Chem., Int. Ed*., 2007, **46**, 5549; (e) S. J. Lee, S. S. Lee, M. S. Lah, J.-M. Hong and J. H. Jung, *Chem. Commun*., 2006, 4539; (f) S. H. Kim, J. S. Kim, S. M. Park and S.-K. Chang, *Org. Lett*., 2006, **8**, 371.

13 H. S. Jung, P. S. Kwon, J. W. Lee, J. I. Kim, C. S. Hong, J. W. Kim, S. Yan, J. Y. Lee, J. H. Lee, T. Joo and J. S. Kim, *J. Am. Chem. Soc*., 2009, **131**, 2008.

14 Hydrogen Sulphide, World Health Organization, Geneva, 1981 (Environmental Health Criteria, No. 19).

15 (a) X. Cao, W. Lin and L. He, *Org. Lett*., 2011, **13**, 4716; (b) S. A. Patwardhan, and S. M. Abhyankar, *Colourage*., 1988, **35**, 15; (c) R. E. Gosselin, R. P. Smith and H. C. Hodge, Clinical Toxicology of Commercial Products, 5th ed.; Williams and Wilkins: Baltimore, MD, 1984; pp III-198–III-202.

16 R. F. Huang, X. W. Zheng and Y. J. Qu, *Anal. Chim. Acta*., 2007, **582**, 267.

17 (a) S. Balasubramanian and V. Pugalenthi, *Water Research*., 2000, **34**, 4201; (b) M. F. Choi and P. Hawkins, *Anal. Chim. Acta.,* 1997, **344**, 105; (c) F. Maya, J. M. Estela and V. Cerda, *Anal. Chim. Acta*., 2007, **601**, 87; (d) E. A. Guenther, K.S. Johnson and K. H. Coale, *Anal. Chem.,* 2001, **73**, 3481; (e) M. Colon, J. L. Todoli, M. Hidalgo and M. Iglesias, *Anal. Chim. Acta*., 2008, **609**, 160; (f) N. S. Lawrence, R. P. Deo and J. Wang, *Anal. Chim. Acta.,* 2004, **517**, 131; (g) C. Giuriati, S. Cavalli, A. Gorni, D. Badocco and P. Pastore, *Journal of Chromatography A*. 2004, **1023**, 105.

18 (a) X. Cao, W. Lin and L. He, *Org. Lett.,* 2011, **13**, 4716; (b) D. Jimenez, R. Martinez-Ma˜nez, F. Sancenon, J. V. Ros-Lis, A. Benito and J. Soto, *J. Am. Chem. Soc*., 2003, **125**, 9000.

19 (a) R. Martinez-Ma˜nez and F. Sancenon, *Chem. Rev*., 2003, **103**, 4419; (b) E. J. O'Neil and B. D. Smith, *Coord. Chem. Rev*., 2006, **250**, 3068.

20 (a) X. D. Lou, J. G. Qin and Z. Li, *Analyst*, 2009, **134**, 2071; (b) S. Rochat and K. Severin, *Chem. Commun*., 2011, **47**, 4391; (c) J. S. Wu, R. L. Sheng, W. M. Liu, P. F. Wang, J. J. Ma, H. Y. Zhang and X. Q. Zhuang, *Inorg. Chem*., 2011, **50**, 6543; (d) L. Zhang, X. Lou, Y. Yu, J. Qin and Z. Li, *Macromolecules,* 2011, **44**, 5186; (e) D. P. Pluth, M. R. Chan, L. E. McQuade and S. J. Lippard, *Inorg. Chem*., 2011, **50**, 9385; (f) J. Chen, Y. Li, W. Zhong, Q. Hou, H. Wang, X. Sun, and P. Yi, *Sensors and Actuators B*., 2015, **206**, 230; (g) Q. Zhou, Y. Zhu, P. Sheng, Z. Wu, and Q. Cai, *RSC Adv*., 2014, **4**, 46951; (h) F. Hou, J. Cheng, P. Xi, F. Chen, L. Huang, G. Xie, Y. Shi, H. Liu, D. Bai and Z. Zeng, *Dalton Trans*., 2012, **41**, 5799; (i) C. Gao, X. Liu, X. Jin, J. Wu, Y. Xie, W. Liu, X. Yao and Y. Tang, *Sensors and Actuators B*., 2013, **185**, 125; (j) C. Kar, M. D. Adhikari, A. Ramesh and G. Das, *Inorg. Chem*., 2013, **52**, 743; (k) L. Tang, M. Cai, Z. Huang, K. Zhong, S. Hou, Y. Bian and R. Nandhakumar, *Sensors and Actuators B*., 2013, **185**, 188.

21 (a) K. Sasakura, K. Hanaoka, N. Shibuya, Y. Mikami, K. Kimura, T. Komatsu, T. Ueno, T. Terai, H. Kimura and T. Nagano, *J. Am. Chem. Soc.,* 2011, **133**, 18003; (b) F. P. Hou, L. Huang, P. X. Xi, J. Cheng, X. F. Zhao, G. Q. Xie, Y. J. Shi, F. J. Cheng, X. J. Yao, D. C. Bai and Z. Z. Zeng, *Inorg. Chem*., 2012, **51**, 2454.

22 A. K. Mahapatra, S. K. Manna, D. Mandal and C. D. Mukhopadhyay, *Inorg. Chem*., 2013, **52**, 10825.

23 (a) A. K. Mahapatra, S. K. Manna, S. K. Mukhopadhyay and A. Banik, *Sensors and Actuators B*., 2013, **183**, 350; (b) A. K. Mahapatra, J. Roy, P. Sahoo, S. K. Mukhopadhyay and A. Chattopadhyay, *Org. Biomol. Chem*., 2012, **10**, 2231; (c) A. K. Mahapatra, S. K. Manna, C. D. Mukhopadhyay and D. Mandal, *Sensors and Actuators B*., 2014, **200**, 123; (d) A. K. Mahapatra, S. K. Manna, K. P. Maiti, R. K. Maji, C. D. Mukhopadhyay, D. Sarkar and T. K. Mondal, *RSC Adv*., 2014, **4**, 36615.

24 (a) X. Zhang, Y. Xiao and X. Qian, *Angew. Chem., Int. Ed.,* 2008, 47, 8025; (b) X. Peng, J. Du, J. Fan, J. Wang, Y. Wu, J. Zhao, S. Sun and T. Xu, *J. Am. Chem. Soc*., 2007, **129**, 1500; (c) Z. Zhang, D. Wu, X. Guo, X. Qian, Z. Lu, Q. Xu, Y. Yang, L. Duan, Y. He and Z. Feng, *Chem. Res. Toxicol*., 2005, **18**, 1814; (d) A. Helal, M. H. O. Rashid, C.-H. Choi and H.-S. Kim, *Tetrahedron,* 2012, **68**, 647.

25 H. S. Jung, J. H. Han, Y. Habata, C. Kang and J. S. Kim, *Chem. Commun.,* 2011, **47**, 5142.

26 Bruker. APEX2, SAINT and SADABS. Bruker AXS Inc.: Madison, WI, USA, 2009.

27 (a) J.-S. Wu, W.-M. Liu, X.-Q. Zhuang, F. Wang, P.-F. Wang, S.-L. Tao, X.-H. Zhang, S.-K. Wu and S.-T. Lee, *Org. Lett.*, **2007**, **9**, 33; (b) A. Z. Weller, *Elektrochem.,* 1956, **60**, 1144. (c) A. Weller, *Prog. React. Kinet.,* 1961, **1**, 188.

28 (a) J. Cheng, X. Ma, Y. Zhang, J. Liu, X. Zhou and H. Xiang, *Inorg. Chem*., 2014, **53**, 3210; (b) L. Wang, W. Qin and W. Liu, *Inorg. Chem. Commun*., 2010, **13**, 1122; (c) J. Wu, W. Liu, J. Ge, H. Zhang and P. Wang, *Chem. Soc. Rev*., 2011, **40**, 3483.

29 (a) Y. Zhou, F. Wang, Y. Kim, S.-J. Kim and J. Yoon, *Org. Lett*. 2009, **11**, 4442; (b) Z. Xu, Y. Xiao, X. Qian, J. Cui and D. Cui, *Org. Lett*., 2005, **7**, 889; (c) T. Gunnlaugsson, J. P. Leonard and N. S. Murray, *Org. Lett*., 2004, **6**, 1557; (d) L. Tang, P. Zhou, K. Zhong and S. Hou, *Sensors and Actuators B*., 2013, **182**, 439.

30 K. C. Ko, J.-S. Wu, H. J. Kim, P. S. Kwon, J. W. Kim, R. A. Bartsch, J. Y. Lee and J. S. Kim, *Chem. Commun.,* 2011, **47**, 3165.

31 R. K. Pathak, V. K. Hinge, A. Rai, D. Panda and C. P. Rao, *Inorg. Chem*., 2012, **51**, 4994.

32 (a) A. D. Becke, *J. Chem. Phys*., 1993**, 98**, 5648; (b) C. Lee, W. Yang and R. G. Parr, *Phys. Rev. B.,* 1988, **37**, 785; (c) D. Andrae, U. Haeussermann, M. Dolg, H. Stoll and H. Preuss, *Theor. Chim. Acta.,* 1990**, 77**, 123.

33 P. J. Hay and W. R. Wadt, *J. Chem. Phys.,* 1985, **82**, 299.

34 (a) R. K. Harris and P. Jackson, *J. Phys. Chem. Solids.,* 1987, **48**, 813; (b) T. H. Lu., P. Chattopadhyay, F. L. Liao and J. M. Lo, *Anal. Sci*., 2001, **17**, 905; (c) K. R. Anumula, *Anal. Biochem*., 2006, **350**, 1.

35 H. S. Jung, J. H. Han, Z. H. Kim, C. Kang and J. S. Kim, *Org. Lett*., 2011, **13**, 5056.

36 M. J. Frisch, G. W. Trucks, H. B. Schlegel, G. E. Scuseria, M. A. Robb, J. R. Cheeseman, G. Scalmani, V. Barone, B. Mennucci, G. A. Petersson, H. Nakatsuji, M. Caricato, X. Li, H. P. Hratchian, A. F. Izmaylov, J. Bloino, G. Zheng, J. L. Sonnenberg, M. Hada, M. Ehara, K. Toyota, R. Fukuda, J. Hasegawa, M. Ishida, T. Nakajima, Y. Honda, O. Kitao, H. Nakai, T. Vreven, J. A. Montgomery, Jr., J. E. Peralta, F. Ogliaro, M. Bearpark, J. J. Heyd, E. Brothers, K. N. Kudin, V. N. Staroverov, T. Keith, R. Kobayashi, J. Normand, K. Raghavachari, A. Rendell, J. C. Burant, S. S. Iyengar, J. Tomasi, M. Cossi, N. Rega, J. M. Millam, M. Klene, J. E. Knox, J. B. Cross,V. Bakken, C. Adamo, J. Jaramillo, R. Gomperts, R. E. Stratmann, O. Yazyev, A. J. Austin, R. Cammi, C. Pomelli, J. W. Ochterski, R. L. Martin, K. Morokuma, V. G. Zakrzewski, G. A. Voth, P. Salvador, J. J. Dannenberg, S. Dapprich, A. D. Daniels, O. Farkas, J. B. Foresman, J. V. Ortiz, J. Cioslowski, and D. J. Fox, Gaussian 09, Revision D.01, Gaussian, Inc., Wallingford CT, 2013.